DOI: 10.1002/anie.201203746

Photochemistry

Probing the Barrier for Internal Rotation of the Retinal Chromophore**

*Yoni Toker, Annette Svendsen, Anastasia V. Bochenkova, and Lars H. Andersen**

Potential barriers which alter the energy spectrum to a certain degree of freedom markedly influence the corresponding contribution to the heat capacity. Heat capacity measurements may hence probe properties of the ground-state internal dynamics of an isolated molecule. Of particular interest is here the hindered internal rotation of the so-called β-ionone ring in the retinal protonated Schiff base (RPSB, see Figure 1) which has a strong impact on the intrinsic photophysical properties of this biological chromophore, important in vision.[1]

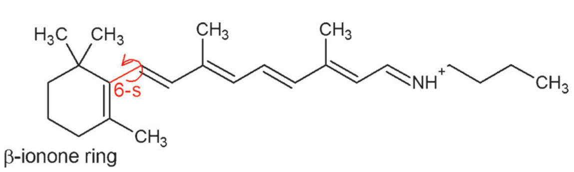

Figure 1. Structure of the *N*-butyl all-*trans* retinal protonated Schiff base.

A flat potential-energy surface (PES) around certain minima, and relatively low barriers for internal rotation, may pave the way for fine-tuning the RPSB photoabsorption by the protein environment. Indeed, the same 11-*cis* RPSB chromophore lies in the center of rod and cone pigments, responsible for human night and color vision, and yet the absorption maxima vary from 425 to 560 nm.[2] Remarkably, our recent gas-phase measurements of the RPSB photoabsorption have shown a flat profile in the range of $\lambda = 530$–610 nm,[3] which is closer to the absorption of the majority of the proteins than to the absorption in solution. Furthermore, the retinal β-ionone ring plays a crucial role in the activation of visual proteins by the all-*trans* retinal agonist formed as a product of the RPSB photoinduced isomerization followed by a Schiff-base linkage hydrolysis. While retaining the 6s-*cis* conformation, the torsion angle changes on average from −65° in the dark state to −32° in the pre-activated meta I state as evident from solid-state NMR spectral analysis.[4] The newly resolved X-ray structure of the constitutively active rhodopsin shows the same trend in the angle change upon activation.[5] The negative twist of the retinal β-ionone ring is −21° in the active meta II state (PDB ID 2X72). Revealing the intrinsic energy profile along the internal rotation of the β-ionone ring in the RPSB chromophore therefore shines light on molecular mechanisms by which the proteins modulate the retinal conformation as well as respond to its alternation.

The aim of this article is two-fold. First, a novel technique for obtaining the heat capacity of isolated charged biological chromophores is demonstrated experimentally and validated theoretically. Second, we discuss its potential application to establish barrier heights of the ground-state potential-energy function that hinders internal rotation like that of the β-ionone ring in the RPSB chromophore.

The problem of measuring the heat capacity of a system which is much smaller than typical thermometers is overcome by using the ion itself. The methodology, similar to that used in cluster science[6–8] is comprised of three steps:

- Equilibrating the ions to a given temperature, T, through collisions with a buffer gas.
- Excitation of the ions with a well-defined energy.
- Measuring the energy and temperature dependence of a certain property, which we refer to as the “calorimetric probe”, of the hot ions.

By correlating changes in temperature, ΔT, to changes in energy transferred to the ion, ΔE, one can extract the heat capacity $C = \Delta E/\Delta T$. Different excitation schemes may be used including photoabsorption, collisional excitation, and atom attachment.[7] The most commonly used calorimetric probe is the fragmentation pattern.

Following photoabsorption, molecules often undergo fast internal conversion and rapid internal vibrational energy redistribution. The internal conversion can involve isomerizations, and does indeed in the case of the RPSB ion. Provided that this energy is not dissipated through collisions with other molecules, or through radiative cooling, the ions dissociate on the ground-state PES on long time scales ranging up to tens of milliseconds, a phenomenon known as delayed fragmentation.[9–11] The amount of ions that dissociate

---

[*] Dr. Y. Toker, Dr. A. Svendsen, Dr. A. V. Bochenkova, Prof. L. H. Andersen
Department of Physics and Astronomy
Aarhus University, Aarhus (Denmark)
E-mail: lha@phys.au.dk
Dr. A. V. Bochenkova
Department of Chemistry

Moscow state University, Moscow (Russia)

[**] We are grateful to M. Sheves and A. A. Granovsky for insightful discussions. We also thank A. V. Abramenkov for an access to a code for solving the Schrödinger equation for internal rotations (periodic potential). This work is supported by the Lundbeck Foundation, the Carlsberg Foundation, the Danish Research Agency, and the Marie Curie European Career Integration Grant within the 7th European Community Framework Programme. A.V.B. acknowledges support from the RFBR (grant number 11-03-01214).

Supporting information for this article is available on the WWW under http://dx.doi.org/10.1002/anie.201203746.

depends on dynamic properties such as the cross-section for photoabsorption and the quantum yields for internal conversion. The time dependence of the decay, however, is independent of these quantities, rather it is a function of the total internal energy of the molecule, which can be transferred to it as heat or as tunable photon energy. We therefore suggest that the time dependence of fragmentation may serve as a sensitive calorimetric probe.

The concept is illustrated in Figure 2. As a first step, chromophore ions are equilibrated to a given temperature in the electronic ground state. The probability for each ion to bear a certain amount of the total thermal energy, ε, residing in vibrations is given by the canonical distribution function $G(\varepsilon, T) = \rho(\varepsilon)e^{-\varepsilon/k_B T}/Q(T)$, where $\rho(\varepsilon)$ is the density of vibrational states, $Q(T)$ the vibrational partition function, and k_B is the Boltzmann constant. Following the initial equilibration to a given temperature T, ions are kept under vacuum conditions, and consequently the total internal energy of each ion is conserved. The ions are then excited by photons of well-defined and tunable energy, resulting in a parallel shift of the initial canonical distribution to higher energies. In other words, the ground-state molecular fragmentation proceeds in a set of microcanonical ensembles with total energies distributed according to the shifted initial distribution.

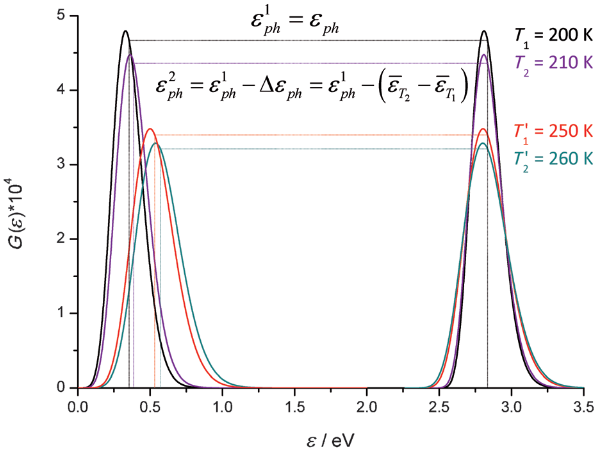

Figure 2. Normalized total vibrational energy distributions of the RPSB chromophore at different temperatures and the same canonical distributions shifted by well-defined photon energies. Dashed lines indicate average energies. Quantum harmonic oscillators are used in the calculations.

Given two measurements at different initial temperatures, T_1, T_2, and photon energies, ε^1_{ph}, ε^2_{ph}, one can adjust the energies to give the same fragmentation rate. Temperature steps ΔT are chosen to be small enough to resolve a temperature dependence of the vibrational heat capacity.

By definition, the vibrational contribution to the heat capacity is related to changes in the *average* internal energy residing in vibrations. Therefore, changes in photon energies $\Delta\varepsilon_{ph}$ are assumed to be equal to changes in average thermal energies. Whereas photoexcitation merely shifts the initial distribution, an increase in temperature not only shifts the energy distribution, but also broadens it. Thus it is not self-evident that one can directly correlate changes in temperature to changes in energy. A mathematical analysis, presented in the Supporting Information, however shows that this approach is valid if certain conditions are satisfied. The first requirement is that the photon energy is much larger than the width of the vibrational energy distribution. In practice this means that "high" temperatures cannot be probed by "low" energy photons. The second condition requires that the change in the variance of the energy distribution with temperature is not large. This condition can be satisfied by choosing small temperature steps. Further conditions which relate to changes in higher statistical moments of the energy distribution, can be neglected.

In the current setup the RPSB cations are produced in an electrospray ion source. After production, the ions are accumulated and thermalized in a multi-pole ion trap through collisions with a helium buffer gas. The temperature of the buffer gas, and thus of the ions, is varied by cooling the trap with liquid nitrogen. To minimize heating of the ions by collisions with helium during extraction from the trap, a pulsed valve is used. Helium is let into the trap for a period of 20 ms to facilitate accumulation and thermalization of the ions. The valve is then closed for 80 ms to allow the helium to be pumped out of the trap, such that at the moment of extraction the pressure within the trap is lower than during accumulation. At a rate of 10 Hz the ions are extracted from the trap and accelerated to 22 keV, after which they are injected into the electrostatic ion storage ring, Aarhus (ELISA). The ions are irradiated 5 ms after injection into ELISA by a visible nanosecond laser pulse. Since the timescales for infrared (IR) radiative cooling and heating have been found to be on the second time scale,[12–14] one can assume that in the period between injection into the ring and probing by the laser the initial energy distribution does not change significantly. Neutral fragments produced by photoabsorption are not affected by the ring deflectors, therefore exit the ring and are counted using a multi-channel plate (MCP) detector.

A power law $I(t) = I_D t^{-d}$ is used to fit the multi-exponential decay[10] of the neutral fragments recorded by the MCP. The use of a power law is counterintuitive since it has no typical timescale associated with it. In the particular case of RPSB the more excited the system is, the smaller is d, which means that the decay is faster at early times (connected to the fact that more excited ions decay faster), but then slower at long times. The exponent d is used in this work as the calorimetric probe.

The temperature was varied in the range from −100 to −10 °C. For each temperature the wavelength was scanned in the region of $\lambda = 500$–600 nm, which corresponds to photon energies of 2.1–2.5 eV. Importantly, our approach does not depend on the absorption cross-section at a particular wavelength. On the left side of Figure 3 a 3D representation of the extracted exponent d is shown as a function of both temperature and photon energy.

The heat capacity is derived from contour lines along the surface depicted in Figure 3 on the left side. Along a contour line, the calorimetric probe, d, remains constant, and thus one

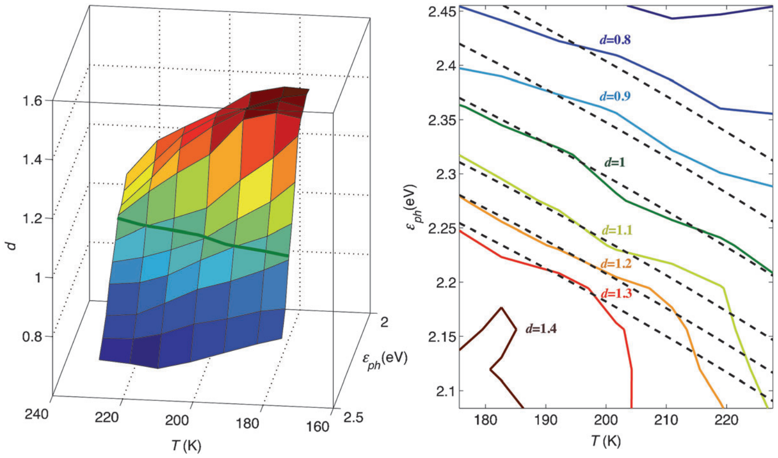

Figure 3. Left side: Fitted exponent *d* as a function of temperature and photon energy. Right side: The colored lines represent contour lines of the surface. The dashed black lines represent the contour lines expected from theory.

can correlate changes in energy to changes in temperature. Figure 3 on the right side shows these contour lines compared to those derived from a theoretical caloric curve.[15] For photon energies above 2.2 eV, the agreement between experiment and theory is good. This correlates precisely with our general theoretical consideration of the applicability limits discussed above.

The red lines in Figure 4 represent the heat capacity derived from a quadratic fit to the contour lines which are shown in Figure 3 on the right side. The heat capacity is notably much smaller than the classical harmonic high-temperature limit of $(3N-6)\,k_B = 183\,k_B$. Fitting all the contour lines leads to a slope of $C/T = (0.16 \pm 0.03)\,k_B/\mathrm{K}$, while the slope expected from theory is $0.15\,k_B/\mathrm{K}$. Notably, the contour line corresponding to $d = 1$ matches the theoretical expectation well. Deviations from theory are seen at low photon energies, in correspondence with the requirement that the photon energy should be higher than the variance in the energy distribution. Discrepancies might also be expected to be caused by the use of the harmonic approximation as well as treating a number of internal rotations as vibrations.

The good correspondence between experiment and theory is a necessary step for establishing our technique as a useful tool for the study of isolated biomolecules. We will now outline some perspectives of this technique, where the next planed step is to compare the heat capacity of RPSB to that of a similar derivative in which the β-ionone ring is chemically locked. By subtracting the two heat capacities (see section D in the Supporting Information) it is possible to isolate the contribution to the heat capacity of a single degree of freedom, namely that of the β-ionone ring rotation. As shown in the following, one can extract the barrier energy of the rotation from this contribution.

For a derivation of the expected heat capacity of the single degree of freedom corresponding to the internal twisting of the β-ionone ring, we have calculated the potential associated with this degree of freedom, which is shown in Figure 5. Three minima on the relaxed PES correspond to the skewed 6s-*cis* (A and A′) and nearly planar 6s-*trans* (C) conformations of the RPSB chromophore. The asymmetry of the potential-energy curve is related to the half-chair conformation of the β-ionone ring itself, which is assumed to be fixed at temperatures relevant to the present studies. A number of articles have been devoted to the study of the relative energies of the 6s-*cis* and 6s-*trans* conformers using different levels of theory.[16] Here a highly accurate fully relaxed MP2/cc-pVTZ profile followed by single-point energy MRMP2/cc-pVTZ corrections[17] along the entire path is used to derive the heat capacities of all conformers. The barrier height ΔE_0, calculated as the difference between the maximum value of the potential and the zero-energy level of the global minimum equals 1059 cm^{-1}. From this one can define a characteristic temperature, T_{FR}, of a hindered to free internal rotation transition as: $T_{FR} = \Delta E_0/k_B = 1524$ K.

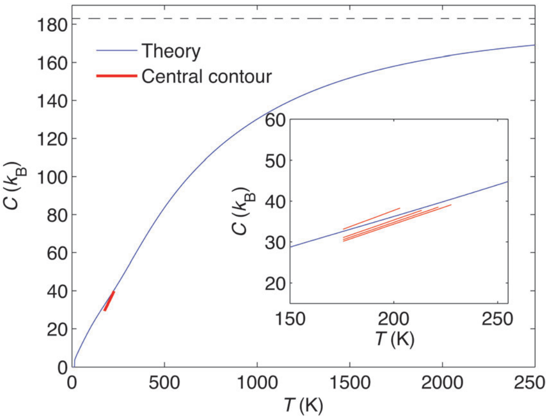

Figure 4. The calculated vibrational heat capacity of the RPSB compared to the one measured in this work. The different red lines correspond to heat capacities derived from the different contour lines shown in Figure 3 on the right side.

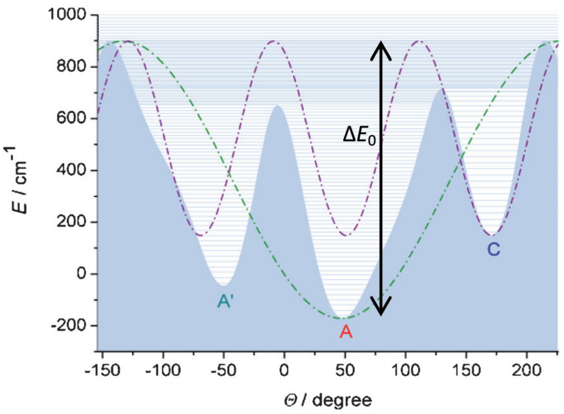

Figure 5. The MRMP2/cc-pVTZ potential-energy profile as a function of the angle *Θ* of the RPSB β-ionone ring. The dashed lines correspond to two model potentials. Note the change in level density at the barrier tops.

The quantum heat capacity derived from the eigenvalues of the one-dimensional internal rotation problem is shown by the solid lines in Figure 6. As explained in section B in the Supporting Information, the curves exhibit the characteristic features one expects for a hindered internal rotator, which include an initial rapid rise of the heat capacity from $0\,k_B$ to $1\,k_B$ (occurring for $T < 100$ K), then a further increase in the heat capacity until a maximum is reached at an intermediate temperature, which we denote as T_m, and finally a decrease of the heat capacity towards the high-temperature limit of $1/2\,k_B$. Remarkably, T_M is well below the characteristic temperature, T_{FR}. Furthermore, it is very close to room temperature and easily accessible experimentally.

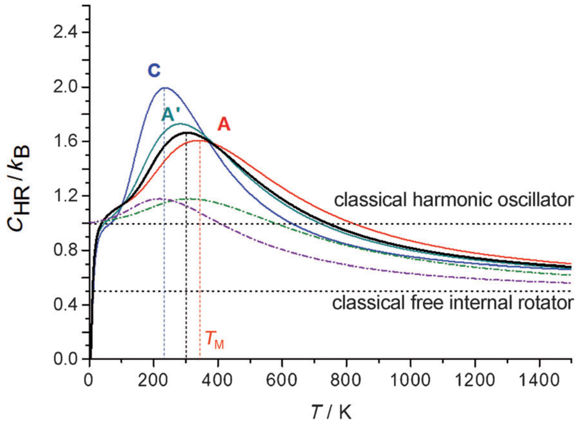

Figure 6. Solid lines: Derived quantum heat capacities of the single degree of freedom associated with rotation of the β-ionone ring. The red, green, and blue solid lines represent the heat capacities of the different conformers (A, A′ and C), and the black solid line represents a heat capacity averaged with Boltzmann factors over all conformers. Dashed lines: classical heat capacities derived from the model potentials shown in Figure 5.

In the following we claim that by measuring T_M one can extract the barrier energy for internal rotation ΔE_0, since the two quantities are correlated. For this purpose we have calculated separately the heat capacity of the three different conformations of the RPSB. This was done by assigning the calculated energy levels to belong to a certain conformer or to a set of conformers depending on the probability function in configuration space for each eigenstate. The corresponding calculated heat capacities of the A, A′ and C conformations are presented as the red, green and blue solid lines, respectively, in Figure 6. Thus, the T_M of the lowest energy conformation, A, is indeed the highest, while for the highest energy conformation, C, T_M is lowest. The total heat capacity, shown by the black line, corresponds to an average value of the heat capacity at each temperature based on the assumption that conformers exist under equilibrium. The corresponding T_M is in between the T_M values of the different conformers.

One does not need high-level computations, such as the ones presented above, to relate T_M to ΔE_0. We propose a classical approach with a simple model potential shown in Equation (1),

$$U = U_0(1-\cos(n\alpha))/2, \tag{1}$$

where the barrier height U_0 is an adjustable parameter related to the highest energy barrier for each conformer, and n determines the number of minima. Model potentials of this form are shown as the dashed lines in Figure 5. The classical heat capacity derived from the two model potentials is shown by the dashed lines in Figure 6. This simple approach reproduces the main features of the heat capacity curve, except for the decrease towards zero at low temperatures, which is a quantum effect. Although the maximal height of the heat capacity is underestimated, the classical calculations give a good approximation of T_M. Importantly, T_M for the heat capacity averaged over all conformations (which is experimentally relevant) is almost identical with the T_M of the classical model based on the simple potential curve (dashed green line in Figure 5).

In summary, we have introduced a novel experimental technique for measuring the heat capacity of an isolated molecular ion. The technique has been applied to the protonated retinal Schiff base chromophore which is central to mammalian color vision. The approach may pave the way for a new field of molecular ion calorimetry, and provide a tool for determining internal barrier energies for conformational changes.

Received: May 15, 2012
Revised: July 10, 2012

Keywords: ab initio calculations · calorimetry · chromophores · conformation analysis · photochemistry

[1] a) A. Lewis, *Proc. Natl. Acad. Sci. USA* **1978**, *75*, 549; b) D. Baylor, *Proc. Natl. Acad. Sci. USA* **1996**, *93*, 560; c) S. T. Menon, M. Han, T. P. Sakmar, *Physiol. Rev.* **2001**, *81*, 1659.
[2] S. L. Merbs, J. Nathans, *Nature* **1992**, *356*, 433.
[3] J. Rajput, D. Rahbek, L. H. Andersen, A. Hirshfeld, M. Sheves, P. Altoè, G. Orlandi, M. Garavelli, *Angew. Chem.* **2010**, *122*, 1834; *Angew. Chem. Int. Ed.* **2010**, *49*, 1790.
[4] M. F. Brown, G. F. J. Salgado, A. V. Struts, *Biochim. Biophys. Acta Biomembr.* **2010**, *1798*, 177.
[5] J. Standfuss, P. C. Edwards, A. D'Antona, M. Fransen, G, Xie, D. D. Oprian, G. F. X. Schertler, *Nature* **2011**, *471*, 656.
[6] A. Aguado, M. F. Jarrold, *Annu. Rev. Phys. Chem.* **2011**, *62*, 151, and references therein.
[7] M. Schmidt, H. Haberland, *C. R. Phys.* **2002**, *3*, 327, and references therein.
[8] M. Vogel, K. Hansen, A. Herlet, L. Schweikard, *J. Phys. B* **2003**, *36*, 1073.
[9] S. B. Nielsen, J. U. Andersen, J. S. Forster, P. Hvelplund, B. Liu, U. V. Pedersen, S. Tomita, *Phys. Rev. Lett.* **2003**, *91*, 048302.
[10] L. H. Andersen, H. Bluhme, S. Boyé, J. D. Jørgensen, H. Krogh, I. B. Nielsen, S. Brønsted Nielsen, A. Svendsen, *Phys. Chem. Chem. Phys.* **2004**, *6*, 2617.
[11] K. Hansen, J. U. Andersen, P. Hvelpund, S. P. Møller, U. V. Pedersen, V. V. Petrunin, *Phys. Rev. Lett.* **2001**, *87*, 123401.

[12] R. C. Dunbar, *Mass Spectrom. Rev.* **1992**, *11*, 309, and references therein.
[13] Y. Toker, O. Aviv, M. Eritt, M. L. Rappaport, O. Heber, D. Schwalm, D. Zajfman, *Phys. Rev. A* **2007**, *76*, 053201.
[14] R. C. Dunbar, *Mass Spectrom. Rev.* **2004**, *23*, 127.
[15] Vibrational analysis has been carried out in the harmonic approximation using the PBE0/cc-pVDZ functional.
[16] K. Bravaya, A. Bochenkova, A. Granovsky, A. Nemukhin, *J. Am. Chem. Soc.* **2007**, *129*, 13035, and references therein.
[17] Calculations were carried out in the frame of the firefly quantum chemistry package: A. A. Granovsky, version 7.1.G, http://classic.chem.msu.su/gran/firefly/index.html.